J Biosci (2019) 44:140
DOI: 10.1007/s12038-019-9953-8

Biophysical methods for quality evaluation of decellularized and recellularized tissue-engineered constructs of organs and tissues

Elena Alexandrovna Gubareva[1], Elena Vyacheslavovna Kuevda[1], Alexander Alexandrovich Basov[1,2], Aleksandr Sergeevich Sotnichenko[1], Sergey Nikolaevich Bolotin[2] and Stepan Sergeevich Dzhimak[2]*

[1]*Kuban State Medical University, Krasnodar, Russian Federation*

[2]*Kuban State University, Krasnodar, Russian Federation*

**Corresponding author (Email, 013194@mail.ru)*

MS received 20 December 2018; accepted 7 August 2019; published online 25 October 2019

Tissue engineering is rapidly growing now and can become a promising alternative to transplantation of organs and tissues, as it is devoid of major shortcomings of transplantology, such as acute shortage, complexity of selection, delivery and storage of donor material, lifelong immunosuppressive therapy. One of the most widely known methods of obtaining biological scaffolds for the subsequent creation of tissue-engineered constructs of organs and tissues is decellularization. The evaluation of the quality of the obtained scaffolds, based on the study of the viability of cell structures in decellularized and recellularized matrices, is one of the priorities of modern regenerative medicine worldwide. In this investigation, the biophysical criteria of decellularization and recellularization of tissue-engineered constructs based on the evaluation of the generation of free radicals in native, decellularized and recellularized tissues by EPR spectroscopy and chemoluminescence in a complex assessment of the quality of biological matrixes obtained are considered using intrathoracic organs and tissues of rats. It has been established that the intensity indices of free radical generation in native and recellularized tissues of animal organs, as well as in decellularized matrices, can serve as one of the express criteria for quantitative assessment of cell structures viability.

Keywords. Chemoluminescence; decellularization; EPR spectroscopy; recellularization; tissue-engineered constructs

1. Introduction

Immunity is an integrative system of the body that, in cooperation with humoral and nervous systems, can effectively maintain homeostasis with the help of unique mechanisms of immune reactivity and immune tolerance (Rackham and Jones 2018; Liu *et al.* 2018; Gauthier *et al.* 2018; Sehati *et al.* 2017). The recent problem of transplantology is the immune rejection that occurs when a recipient's immune system contacts a graft. One of the most promising strategies for solving transplantology problems is tissue engineering, which is at the intersection of biology, physics, chemistry, medicine and biotechnology and is aimed at maintaining, replacing or restoring damaged organs and tissues (Frey *et al.* 2016; Rafati *et al.* 2011). The tissue engineering approach for creating constructs structurally and functionally similar to native organs includes the following components: biomaterials created on the basis of biological or synthetic matrices, cells, bioreactor and biologically active substances, including growth factors, proangiogenic factors, differentiation factors, and others. A promising method for creating natural materials based on acellular matrices is decellularization (Mahla 2016). The main requirements for the resulting decellularized matrices are: biomechanical strength; non-toxicity upon the contact of the body with the material, as well as the products of its degradation; sterility; immunity to infections; the ability to maintain the adhesion and viability of various cell types *in vitro* and the ability to act as a basis for the growth and differentiation of recipient cells *in vivo*, while biocompatible materials should not cause inflammation or rejection, allergy or sensitization, inhibit the healing process, be carcinogenic or cause local complications. Tissue engineered constructs should be subjected to a comprehensive assessment with the establishment of quality criteria for the resulting material.

A number of works have shown the role of free-radical oxidation reactions in the regulation of many biological processes, including those that ensure the vital activity of cells, their growth, differentiation and aging (Kuksal *et al.* 2017; Nastase *et al.* 2017; Stockwell *et al.* 2017; Dzhatdoeva

et al. 2016). Therefore, the study of the intensity of free radicals generation in native, recellularized tissues of internal organs, as well as in their decellularized matrices, can serve as one of the criteria making possible quantitative assessment of cell structures viability, that is, to assess the quality of the performed measures both in tissue decellularization and after matrix recellularization with allogenic or autologous cells, which in general is supposed to increase the effectiveness of these measures. In living cells under physiological conditions, the steady state concentration of free radicals is rather low, however, modern methods for their detection and identification, primarily chemoluminescence and electron paramagnetic resonance (EPR) spectroscopy, make possible to detect them to high precision using precision equipment (Kishikawa *et al.* 2009; Sozarukova *et al.* 2016; Zhang and Weiner 2014). It is known that EPR signals, that can be detected at room temperature in particles (Ito and Hyodo 2016) forming paramagnetic centers, are observed, for example, in the presence of phenoxy or semiquinone radicals in the biological system, including the semiquinone radical ubiquinone (SQ·), which is formed in the mitochondrial respiratory chain (King *et al.* 2009; Brand 2010), which is an essential component of the majority of viable cells (Daneshgar *et al.* 2016). For example, superoxide, which actively produces from mitochondrial respiratory complex III at the ubiquinol oxidation center, and NADPH oxidase-derived reactive oxygen species (ROS) have additional physiological functions as signaling molecules during many cellular processes (Orr *et al.* 2015; Bleier and Dröse 2013), stimulate membrane assays and can be registered by chemoluminescence method in living tissues and cells (Kőszegi *et al.* 2017). Moreover, constant ROS generation is the important part of the native cells (Rezende *et al.* 2017) and chemoluminescence is ideal imaging technique for detecting physiologically relevant variations in ROS concentration (Maulucci *et al.* 2016).

In its turn, the chemoluminescence method is very sensitive for the detection of highly reactive radicals, since it evaluates not the steady-state concentration but the reaction rate in which they are formed (Wang *et al.* 2017; Vladimirov and Proskurnina 2009), which expands, along with the use of EPR-spectroscopy, the possibility of studying various features of free radical oxidation in native, decellularized and recellularized tissues of intrathoracic organs. For example, SQ· levels may be high effectively evaluated in human cells by EPR-spectroscopy (Yamamoto *et al.* 2018; Wang 2016).

In view of the foregoing, the aim of this investigation was to develop a new and effective method for assessing the degree of decellularization of the extracellular matrix and the viability of the cell structures of the recellularized intrathoracic organs and tissues based on the residual DNA quantification, ultrastructural analysis, quantification of the components of the extracellular matrix, the content of paramagnetic centers and features of free radicals generation.

2. Materials and methods

Protocols of experimental animal studies on the basis of the laboratory of fundamental research in the field of regenerative medicine of the Kuban State Medical University were approved by the local ethical committee (Protocol No. 21/1). Before performing surgical interventions, animals were intraperitoneally injected with a lethal dose of barbiturates (150 mg/kg), an injection of heparin at a dose of 100 units was made an hour before the operation. The explantation of organ complexes 'heart-lungs-diaphragm' was performed by a single unit, then, depending on the type of organ, directional decellularization was carried out using a detergent-enzymatic method according to protocols developed earlier (Sotnichenko *et al*. 2013; Gubareva *et al.* 2016). Briefly, organ was perfused with MilliQ water 1 h, then 3 h 4% sodium deoxycholate (Sigma Aldrich, USA), 10 min PBS (Gibco, Life Technologies, USA), 1 h DNase e I 2000 kunitz units (Sigma Aldrich, USA) diluted in PBS with calcium and magnesium (Invitrogen, Life Technologies, USA), and 2 washes of 30 min each of 2 mM EDTA (Sigma Aldrich, USA) in MilliQ water. Tissues were then rinsed for 12 h using PBS (Gibco, Life Technologies, USA). All steps were performed at room temperature, with a reagent final volume of 200 ml.

2.1 *Morphological evaluation of the decellularized matrix*

Samples of native and decellularized rat lungs, heart, diaphragm, and also recellularized lungs were fixed in 10% neutral buffered formalin, dehydrated and paraffinized routinely using the Leica TP1020 automatic histoprocessor (Germany) and the Leica EG1150H modular unit (Germany). Paraffin 5 μm thick sections, obtained by means of the Leica RM2235 rotary microtome (Germany), were dewaxed and hydrated, followed by staining with routine histological stains and fluorophore (4′, 6-diamidino-2-phenylindole) DAPI (Sigma-Aldrich, USA). Extracellular matrix proteins were visualized by immunohistochemical analysis, for which mouse monoclonal antibodies to elastin (ab21610, Abcam, England), type IV collagen (ab6586, Abcam, England), type I collagen (ab34710, Abcam, England) were selected as primary antibodies. The microscopy was studied using the Olympus IX51 microscope (Japan).

2.2 *Morphometric quantitative analysis of the decellularized matrix*

To obtain photomicrographs, the Olympus IX51 microscope with an Olympus XC30 camera was used. Paraffin sections were used as samples with visualized extracellular matrix proteins by means of immunohistochemical staining. The photomicrographs were saved at resolution 2080 × 1544 in

the form of 16-bit images in TIFF format. The following criteria were used for image selection: the randomness of the choice of visual fields, the absence of visual defects and artifacts, uniform illumination of the field of view, the same white balance and exposure parameters for the whole series of photomicrographs. The obtained data were handled with the RawTherapee software for aligning the white balance, where a fragment of the optically empty background area was used as a neutral gray point. The result was saved as 8-bit TIFF files. The images were analyzed in the 'DAB-analyzer' software developed by the authors (*https://github.com/meklon/DAB_analyzer*) with the construction of a summary table of the samples studied indicating the areas of positive staining. According to the obtained data, the content of extracellular matrix proteins in the samples was plotted.

2.3 *DNA quantification*

To quantify the DNA content in native and decellularized organs, as well as in the recellularized ones, standard reagent kits (DneasyBlood and Tissue Kit, Qiagen, Sweden) were used on the NanoDrop ND-1000 spectrophotometer (Thermo Fisher Scientific Inc., USA) using standard manufacturer protocols.

2.4 *Multipotent mesenchymal stromal cells isolation (MMSC)*

In this study, rat MMSC of bone marrow origin were used. Before isolating the cells, experimental animals were injected intraperitoneally with barbiturates in a lethal dose of 150 mg/kg. Femoral and tibial bones were isolated, the metaphyses were cut off, and the bone marrow was washed out with PBS solution using a needle and a syringe into a sterile tube. After centrifugation, the sediment was resuspended in a culture medium (DMEM, Invitrogen, USA) with 10% fetal bovine serum (FBS, Invitrogen, USA) and 1% penicillin and streptomycin (Invitrogen, USA), placed in a culture flask (Corning, USA) and incubated at 37°C and 5% CO2. After 24 hours of incubation, the culture medium was removed, eliminating all non-adherent cells. Cells that adhere to culture flask were identified as MMSC of zero passage. MMSC were cultured to 4-5 passages and used in the subsequent experiments.

Static recellularization of decellularized samples was performed before chemoluminescence and EPR-spectroscopy. 6 mm samples were obtained from the decellularized matrices in sterile conditions and were further sterilized with 10% ethanol solution for 15 minutes and washed twice with PBS +/+ solution with the addition of antibiotic-antimycotic (all Gibco, England) for 15 minutes each time. Recellularization of the obtained samples was carried out in a 96-well plate by placing the cells with a sterile pipettor on a scaffold in an amount of 20,000 MMSC per well within 50 hours.

2.5 *EPR-spectroscopy*

Measurement of the EPR spectra was carried out on a JES FA 300 spectrometer (JEOL, Japan) at a temperature of 24°C in the X range. Measurement parameters: super-high-frequency radiation with a capacity of 1 mW, microwave frequency - 9144 MHz, amplitude of high-frequency modulation −0.1 mT (Gubareva *et al.* 2016). Samples were preliminarily lyophilized in a dryer LS-1000 (Prointech, RF), and then weighed (scales Ohaus, China, accuracy ± 0.01 mg). The EPR signal of the weighted sample was measured in a quartz ampoule (5 mm in diameter), with the sample weight in the cavity zone being 0.0300 g. The integrated intensity of the EPR signal in the samples was calculated by double numerical integration, the concentration of the paramagnetic centers in the samples was determined by comparing the intensity of the received signal with a standard sample signal (TEMPO) containing $6.4 \cdot 10^{-7}$ mole of paramagnetic centers.

2.6 *Chemoluminescence*

The study of free radical oxidation was carried out with the help of the hardware and software complex 'Chemiluminometer Lum-5773' (RF) and specialized software 'PowerGraph 3.x Professional' (Vladimirov *et al.* 2011). The diameter of the lung tissue samples studied was 6.0 ± 0.1 mm, their thickness was 4.0 ± 0.2 mm. In preparation for the study, the background luminescence (BL) of the chemiluminometer was recorded with an empty cuvette compartment (figure 1).

The following parameters were also evaluated: own chemoluminescence area of the bioobject; area of the induced chemoluminescence (ArInC), which was initiated by introducing 0.3% hydrogen peroxide solution (H_2O_2) in a volume of 100 µl into the cuvette; maximum of induced chemoluminescence flash ($InCF_{max}$); rising slope of the induced chemoluminescence flash curve (rSCF), which characterizes the average rate of change in luminescence intensity from the moment of flash initiation of the induced chemoluminescence to achieve $InCF_{max}$; descending slope of the induced chemoluminescence flash curve (dSCF), which characterizes the average rate of change in the intensity of luminescence from $InCF_{max}$ to the end of the detection of the induced chemoluminescence flash.

To standardize the results obtained, both the area of the background luminescence and the own chemoluminescence area of the bioobject were measured for 100 seconds. The own chemoluminescence area of the bioobject in 100 seconds (ArOC) was determined by the formula: $ArOC = ArOC_i\text{-}BL$, where i stands for an individual sample,

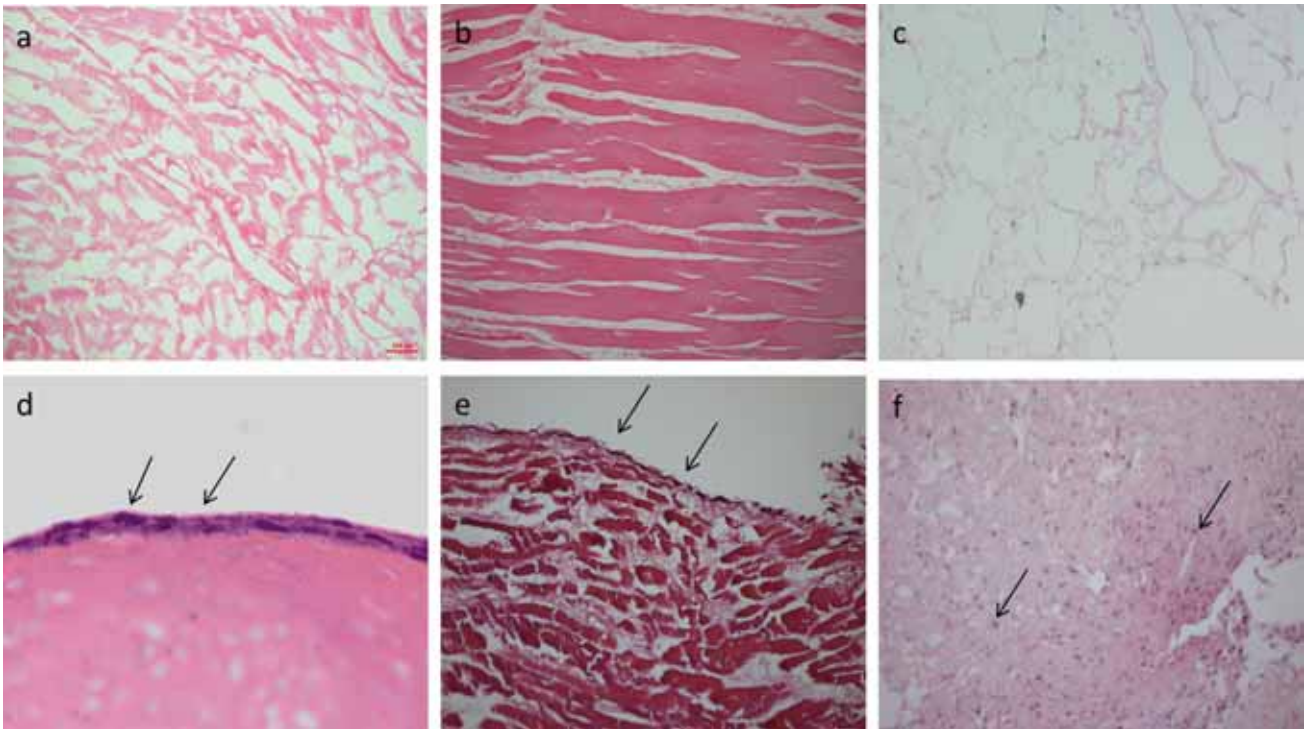

Figure 1. Histological evaluation. Decellularised heart (**a**), diaphragm (**b**), lung (**c**). reseeded heart (**d**), diaphragm (**e**), lung (**f**). hematoxylin and eosin, and an absence of cell nuclei in decellularized organs and MMSC on top of scaffolds.

the result is expressed in volts (V). The area of the induced chemoluminescence (ArInC) was determined by the formula: $ArInC = ArInC_t\text{-}ArOC_t$, where $ArInC_t$ is the area of the induced chemoluminescence of the bioobject in the course of time (t) required for the flash of the induced chemoluminescence to achieve the plateau (the results were expressed in V); $ArOC_t$ is the own chemoluminescence area of the bioobject in the course of time (t), the results obtained are expressed in V; t stands for the duration of the induced chemoluminescence flash before it achieves the plateau (the results obtained were expressed in seconds). The indices were also determined: (1) ArInC·ArOC, which allows to estimate the total generation of free radicals in a native bioobject and in the same bioobject after chemoluminescence induction by introducing H_2O_2, the results were expressed in conventional units; (2) rSCF·dSCF is equal to the product of rSCF and dSCF modulo, which allows to estimate the features of generation of free radicals in the bioobject taking into account the shape of the chemoluminescence plot (ratio to the $InCF_{max}$ point), the results were expressed in conventional units.

2.7 *Statistical analysis*

Statistical processing of the obtained data was carried out using the methods of variation statistics, the results were presented as the median (Me), percentiles 25 and 75 (P_{25} and P_{75}) in case of deviation of the experimental data obtained from the normal Gauss-Laplace law, or as the arithmetic mean (M) and error of the mean (m) for results characterized by the Gauss-Laplace distribution. Reliability of estimate of differences in the mean values found between the groups was carried out using the nonparametric Mann-Whitney U test (for independent groups). Statistically significant differences were assumed those for which the confidence value was $p<0.05$.

3. Results

In a macroscopic analysis of the samples of decellularized heart, lung and diaphragm matrices, it was noted that the tissues after cells removal lost a characteristic dark red color and acquired an opalescent-white color inherent in the decellularized organs (figure 1), which correlates with the literature data (Badylak *et al.* 2011; Ott *et al.* 2008; Wainwright *et al.* 2010; Sellaro *et al*. 2007; Ott *et al.* 2010 Conconi *et al.* 2005). Staining with both hematoxylin and eosin and fluorophore DAPI did not reveal nuclei and cell structures in the matrices after decellularization, demonstrated the architectonics characteristic of the native matrix; moreover, the adventitial membrane of small blood vessels was preserved.

DNA quantification in native and decellularized tissues of the lung, heart and diaphragm showed a significant decrease in DNA content in decellularized matrices (Sotnichenko *et al.* 2013; Gubareva *et al.* 2016; Kuevda *et al.* 2013). Thus, DNA

quantification in native and decellularized lung samples revealed that about 91.2% of nuclear material was removed in the process of decellularization: 15.73 ± 0.07 ng/mg tissue – before and 1.39 ± 0.02 ng/mg tissue – after completion of detergent solutions exposure ($p \leq 0.0001$). At lung recellularization the level of DNA content was 23.6% of the native ($p = 0.0005$) (figure 2).

Immunohistochemical evaluation of the extracellular matrix did not show any qualitative changes in its composition. The main structural proteins – collagen types I and IV, elastin – were found in the decellularized matrices of heart, lungs and diaphragm. At the same time, the morphometric quantitative analysis of the components of the extracellular matrix in the samples of the decellularized lung showed a significant decrease in elastin content: from 70.93% in the native lungs to 0.44% after the completion of the decellularization. The percentage of collagen type I also decreases, while the content of collagen type IV even slightly increases due to sample density increase after exposure to detergents (figure 3).

This reduction in elastin content is consistent with a change in the biomechanical properties of the lung scaffold after decellularization in a study on the model of non-human primates (Kuevda *et al.* 2016).

The EPR spectra of the native heart indicated the highest content of semiquinone radicals with a g-factor value of 2.005 to 2.011. The median signal intensity in the samples of the native heart was 3.9 times higher than that of the native lung and 6.5 times higher than the native diaphragm index (table 1), reflecting the significant activity of free radical processes in the mitochondria of native cardiomyocytes compared to other tissues.

After the decellularization of the rat heart tissues, no paramagnetic centers corresponding to SQ· were detected, which was confirmed by the absence of a signal with a g-factor in the range from 2.005 to 2.011, which would significantly differ in intensity from zero. The data obtained reflect the absence of a system of electron carriers necessary for the functioning of living cells in decellularized heart tissue. The EPR spectra of decellularized tissues of the diaphragm and lung had a similar character (figure 4), which confirmed the absence of viable cells in the relevant organs after the decellularization.

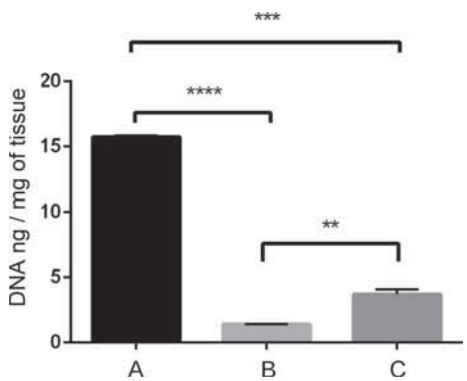

Figure 2. Residual DNA quantification in native (A), decellularized (B) and recellularized (C) rat lungs: **** – $p \leq 0{,}0001$; *** – $p = 0.0005$; ** – $p = 0.007$.

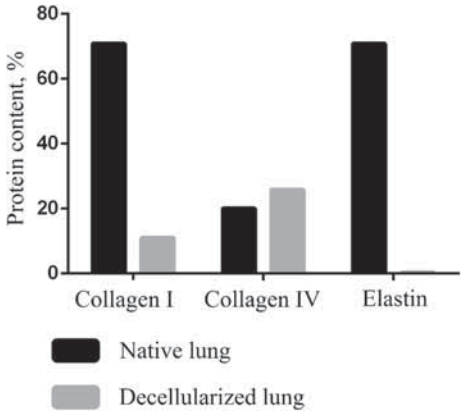

Figure 3. Morphometric quantitative analysis of the components of the extracellular matrix of the decellularized rat lung with representative examples of the morphological and histochemical structure.

Table 1. EPR spectroscopy of native, decellularized and recellularized organs

Bioobject	PMC concentration, $\times 10^{-8}$ mole/g (A)	PMC concentration, $\times 10^{-8}$ mole/g (B)	PMC concentration, $\times 10^{-8}$ mole/g (C)
Me (heart)	48,71 (n = 5)	0,0 (n = 5)	–
P_{25-75}	23,82 – 87,04		
Me (lung)	12,40 (n = 5)	0,0 (n = 4)	2,36 (n = 4)
P_{25-75}	8,52 – 54,93		1,15 – 6,31
Me (diaphragm),	7,53 (n = 5)	0,0 (n = 5)	2,29 (n = 4)
P_{25-75}	4,29 – 9,16		1,84 – 3,97

Note: A – native tissues, B – decellularized tissues, C – recellularized tissues, PMC – paramagnetic centers, Me – median, P – percentile.

In the recellularized matrices of rat lungs, unlike the decellularized ones, the EPR spectroscopy detected radicals corresponding to the semiquinone radical of ubiquinone and indicated the living cell elements in the samples studied. A difference in the intensity of the EPR signal between the tissues of the native and recellularized lung was also established, while the median of the latter was 80.9% less, indicating a lower content of cells in the recellularized lung. Figure 4 presents representative examples of EPR spectra of native, decellularized and recellularized lyophilized lung tissue of certain laboratory animals. When comparing the intensity of the EPR signal of recellularized lung tissues and the diaphragm, there were no significant differences, which may indicate the same survival rate of allogeneic MMSCs on the matrices of these organs.

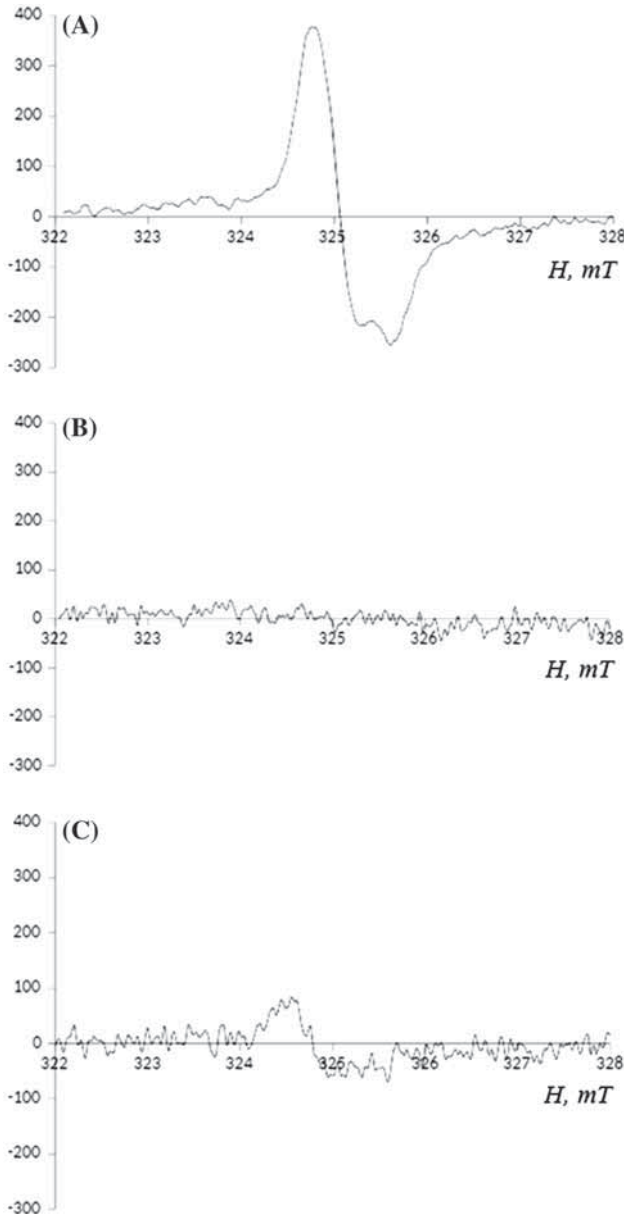

Figure 4. EPR spectra (g = 2.009) of the samples of native (**A**), decellularized (**B**) and recellularized (**C**) lyophilized lung tissue of certain laboratory rats. *Note*: as ordinate – the first derivative of the value of high-frequency radiation to the intensity of the magnetic field absorbed by the sample; as abscissa – strength of the magnetic field.

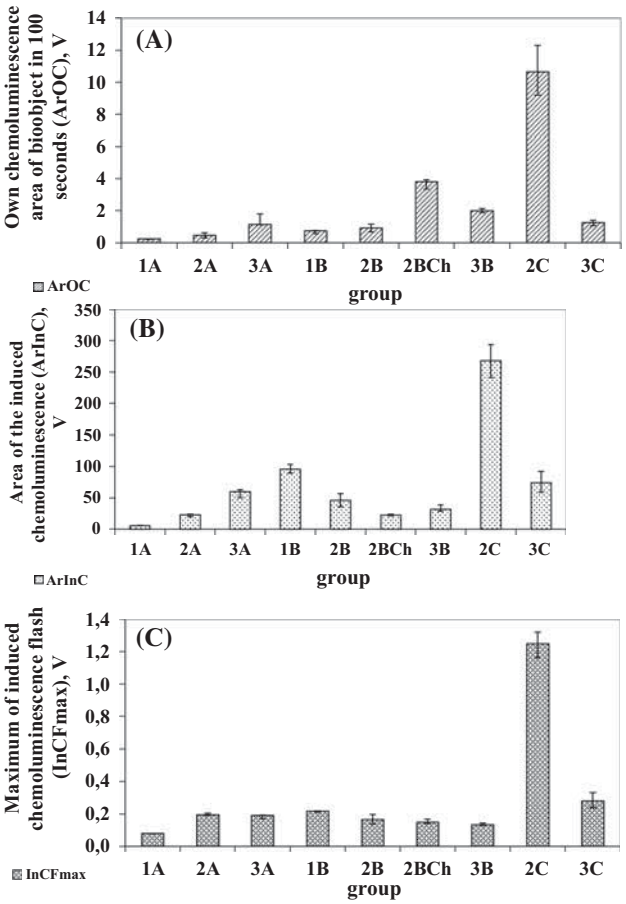

Figure 5. Indices of chemoluminescence of native, decellularized and recellularized organs.

ArOC of native tissues of all studied intrathoracic organs was less than ArOC of decellularized tissues (figure 5A): differences in this indicator were 212% between native and decellularized heart tissues ($p = 0.009$), lungs – 96% ($p = 0.05$) and diaphragm – 75% ($p = 0.016$).

When a 0.3% hydrogen peroxide solution was added to the tissues, an increase in the chemoluminescence area was observed, which was significantly higher in the decellularized heart matrix (18 times) and lung (2 times) compared to similar native samples, while ArInC of the decellularized diaphragm matrix was 47% lower compared to the native tissue (figure 5B). The lower average values of ArOC and ArInC in native heart tissues may be due to a higher number of antioxidant compounds capable of inactivating free radicals in the cardiomyocytes, as compared with the decellularized heart matrix and native tissues of other parenchymal and muscular intrathoracic organs. $InCF_{max}$ in native heart tissues was 2.7 times lower compared with the decellularized matrix, whereas $InCF_{max}$ of the corresponding lung and diaphragm tissues scarcely differed from each other (figure 5C).

The ArInC·ArOC index was significantly increased in the decellularized heart and lung tissues (table 2): 51.3 times ($p = 0.009$) and 3.7 times ($p = 0.014$) respectively higher (compared to the native tissues), in contrast to the ArInC·ArOC index of the diaphragm, which was about the same in its native and decellularized samples ($p = 0.6$). All of the above reflects a sharp decrease in antioxidant protection in the tissues of heart and lung after the decellularization, leading to the prevalence of prooxidant factors (figure 6).

The study showed that the rSCF·dSCF index is always reliably higher in native tissues than in decellularized ones

Table 2. Indices of chemoluminescence of native, decellularized and recellularized organs

	1A (n = 5)			1B (n = 5)			$2B_{Ch}$ (n = 6)		
Index	Me	P 25	P 75	Me	P 25	P 75	Me	P 25	P 75
ArInC·ArOC	1,28	1,11	1,53	65,67	58,53	65,73	83,13	80,36	87,08
rSCF	$4{,}368 \cdot 10^{-3}$	$4{,}367 \cdot 10^{-3}$	$4{,}428 \cdot 10^{-3}$	$8{,}125 \cdot 10^{-4}$	$7{,}784 \cdot 10^{-4}$	$8{,}175 \cdot 10^{-4}$	$1{,}749 \cdot 10^{-3}$	$1{,}637 \cdot 10^{-3}$	$1{,}969 \cdot 10^{-3}$
dSCF	$-7{,}455 \cdot 10^{-5}$	$-8{,}523 \cdot 10^{-5}$	$-7{,}257 \cdot 10^{-5}$	$-1{,}198 \cdot 10^{-4}$	$-1{,}212 \cdot 10^{-4}$	$-1{,}082 \cdot 10^{-4}$	$-8{,}777 \cdot 10^{-5}$	$-9{,}586 \cdot 10^{-5}$	$-8{,}657 \cdot 10^{-5}$
rSCF·dSCF	3,256	3,214	3,723	0,985	0,885	1,207	1,600	1,398	1,754
	2A (n = 5)			2B (n = 4)			2C (n = 4)		
Index	Me	P 25	P 75	Me	P 25	P 75	Me	P 25	P 75
ArInC·ArOC	11,53	7,25	14,33	42,22	25,18	67,15	2788,76	2474,63	3250,13
rSCF	$4{,}629 \cdot 10^{-3}$	$3{,}531 \cdot 10^{-3}$	$4{,}848 \cdot 10^{-3}$	$1{,}256 \cdot 10^{-3}$	$1{,}063 \cdot 10^{-3}$	$1{,}449 \cdot 10^{-3}$	$2{,}641 \cdot 10^{-2}$	$2{,}331 \cdot 10^{-2}$	$2{,}950 \cdot 10^{-2}$
dSCF	$-2{,}730 \cdot 10^{-4}$	$-2{,}768 \cdot 10^{-4}$	$-2{,}64 \cdot 10^{-4}$	$-1{,}133 \cdot 10^{-4}$	$-1{,}698 \cdot 10^{-4}$	$-5{,}677 \cdot 10^{-3}$	$-1{,}249 \cdot 10^{-3}$	$-1{,}457 \cdot 10^{-3}$	$-1{,}041 \cdot 10^{-3}$
rSCF·dSCF	12,732	12,639	13,420	1,426	0,700	1,781	331,214	244,737	431,822
	3A (n = 5)			3B (n = 5)			3C (n = 4)		
Index	Me	P 25	P 75	Me	P 25	P 75	Me	P 25	P 75
ArInC·ArOC	66,81	61,58	89,48	59,45	53,20	76,78	91,10	78,82	97,48
rSCF	$3{,}336 \cdot 10^{-3}$	$2{,}993 \cdot 10^{-3}$	$3{,}743 \cdot 10^{-3}$	$3{,}086 \cdot 10^{-3}$	$2{,}899 \cdot 10^{-3}$	$3{,}132 \cdot 10^{-3}$	$1{,}337 \cdot 10^{-2}$	$1{,}115 \cdot 10^{-2}$	$1{,}559 \cdot 10^{-2}$
dSCF	$-1{,}451 \cdot 10^{-4}$	$-1{,}466 \cdot 10^{-4}$	$-1{,}341 \cdot 10^{-4}$	$-6{,}756 \cdot 10^{-5}$	$-7{,}080 \cdot 10^{-5}$	$-6{,}251 \cdot 10^{-5}$	$-2{,}137 \cdot 10^{-4}$	$-2{,}523 \cdot 10^{-4}$	$-1{,}751 \cdot 10^{-4}$
rSCF·dSCF	4,012	3,566	4,842	2,011	1,888	2,120	26,836	25,297	29,263

Note: 1 – heart, 2 – lung, 3 – diaphragm, A – native tissues, B – decellularized tissues, C – recellularized tissues, Ch – chlorhexidine, Me –median, P – percentile.

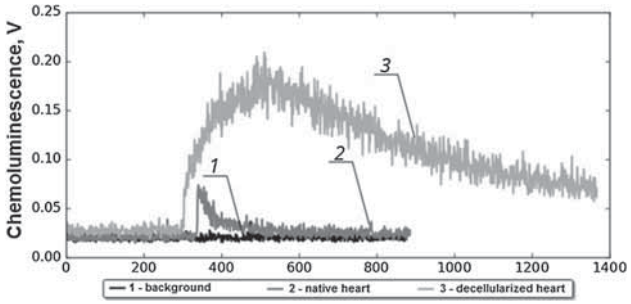

Figure 6. Representative examples of chemoluminescence of native and decellularized heart tissue of certain laboratory rats.

(Table 1.2): 3.3 times in the heart ($p = 0.009$), 8.9 times in the lung ($p = 0.014$), and 2.0 times in the diaphragm ($p = 0.009$); the even higher index rSCF·dSCF is characteristic of the recellularized tissues, which exceed in this index the native tissues: 26.0 times in the lung ($p = 0.014$) and 6.7 times in the diaphragm ($p = 0.014$), which makes possible an objective monitoring the efficiency of decellularization and recellularization in the parenchymal and muscular intrathoracic organs by means of chemoluminescence.

To confirm these statements, the effect of chlorhexidine at a concentration of 1:10 on the chemoluminescence indices of decellularized lung tissues was also studied. The treatment of decellularized lung tissue with chlorhexidine solution demonstrated that the antiseptic increases ArOC by 4.2 times in comparison with the intact tissue of the decellularized lung. At the same time, the area of induced chemoluminescence decreased by 51.5%, and the ArInC·ArOC index increased by 96.9% (table 2).

For recellularized lung tissues treated with chlorhexidine (figure 7), plots of chemoluminescence curves having a similar shape to the curve of the native lung tissue chemoluminescence are characteristic.

In addition, they significantly differed in shape from the chemoluminescence curves of the corresponding decellularized lung tissues treated with chlorhexidine. First of all, these chemoluminescence curves significantly differed in the steepness of rSCF and dSCF (groups 2C and $2B_{Ch}$, table 2). Also, the chemoluminescence plots of lungs treated with an antiseptic after decellularization resembled the chemoluminescence curve of the actual decellularized lung tissue as compared to native and recellularized tissue samples (figure 7), primarily by the nature of the chemoluminescence decay, which was confirmed by the absence of significant differences in dSCF ($p = 0.20$). At the same time, indices characterizing the intensity of H_2O_2-induced chemoluminescence of recellularized scaffolds – ArInC, ArInC·ArOC, $InCF_{max}$ and rSCF·dSCF – significantly differed from the decellularized matrix.

It is important to point out that the revealed pattern of increase in the rSCF·dSCF index in the presence of cells in the tissue under study was preserved: in the treatment of

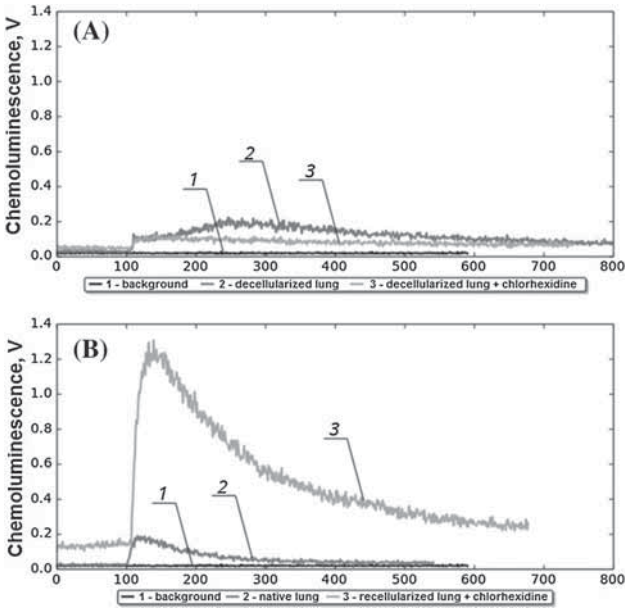

Figure 7. Representative examples of chemoluminescence of decellularized, decellularized and then treated with chlorhexidine solution (**A**), native and recellularized lung tissue (treated with chlorhexidine solution) of certain laboratory rats (**B**).

tissues with chlorhexidine, rSCF·dSCF index in recellularized lung tissues increased by 207.0 times in comparison to the decellularized lung matrix treated with chlorhexidine at the same concentration (table 2).

The existing features of the intensity of the own luminescence of the samples when treated with an antiseptic should be noted: in recellularized lung tissues treated with chlorhexidine, a significant increase in ArOC by 2.8 times was observed, compared with the decellularized matrix ($p = 0.011$) treated with chlorhexidine at the same concentration.

4. Discussion

The results obtained allow us to consider the EPR spectroscopy one of the methods for studying cells viability in native, decellularized and recellularized tissues, since the absence of an EPR signal with the g-factor in the range from 2.005 to 2.011 indicates the absence of living cell structures in the sample under study that is of practical importance for determining the completeness of the stage of preparation of biomatrix, evaluated by the degree of destruction of cell structures in tissues, whereas the presence of this signal confirms the ability of allogeneic cells to survive after matrix recellularization.

In turn, in the samples of the recellularized lung and diaphragm, there was a pronounced increase in all (ArOC, ArInC, $InCF_{max}$, ArInC·ArOC) parameters described above (figure 5; table 2), which may indicate a significant number of viable cells in their recellularized tissues, possessing

increased biochemical activity (Psaltis *et al.* 2013) and probably the ability to generate higher concentrations of free radicals than cells of native tissues, leading to the prevalence of prooxidant factors in the regenerated tissues, which is apparently one of the reasons for the less stability of the recellularized cells, compared to similar native cells, and to unfavorable external influences during their storage or transplantation.

The most significant reliable pattern of changes in the chemoluminescence indices of native, decellularized and recellularized tissues of parenchymal and muscular intrathoracic organs was established when studying the shape of the induced chemoluminescence flash, which is characterized by the steepness of its rising and descending slopes (relative to $InCF_{max}$). For native and recellularized tissues, in all cases studied without exception in this study, a sharper increase and then an accelerated decrease in the induced chemoluminescence flash was observed in comparison with the decellularized tissues.

The increase in ArOC in the chemoluminescence of decellularized lung scaffolds after treatment with chlorhexidine may be due to the luminescence of the matrix upon exposure to chlorhexidine, which is capable of forming hypochlorite and probably leading to the destruction of extracellular antioxidant factors.

In turn, the higher ArInC·ArOC index of recellularized lung tissue treated with chlorhexidine, compared with samples of decellularized lung tissue treated with chlorhexidine at the same concentration, is most likely to confirm the presence of cell structures containing compounds capable of acting as a proton donor (for example, metals of mixed valence and oxidation states: iron, copper, manganese and others) and reduce hydrogen peroxide to a hydroxyl radical. In view of the foregoing, treatment with chlorhexidine may be considered optimal for cells seeded on a scaffold, as evidenced by higher chemoluminescence indices, in particular ArOC, as well as ArInC, $InCF_{max}$, ArInC·ArOC index, reflecting the high metabolic activity of cells.

Thus, the developed method for assessing the degree of decellularization of the extracellular matrix and the viability of the cell structures of the recellularized intra-thoracic organs and tissues, based on the residual DNA quantification, ultrastructural analysis, quantitative evaluation of extracellular matrix components, the content of paramagnetic centers, and the features of free radical generation, has confirmed its effectiveness in experiments on tissues of intrathoracic organs (heart, lung, diaphragm) in rats.

5. Conclusion

On the basis of the conducted studies, it was found that in addition to the conventional morphological control, DNA quantification and the morphometric quantitative analysis of the components of the extracellular matrix (collagen I and IV types, elastin); it is advisable to use biophysical methods to assess the functional state of cell structures. Thus, the EPR-spectroscopy method makes it possible to detect the viable cells in native and recellularized tissues of parenchymal and muscular intrathoracic organs with a concentration of paramagnetic centers with a g-factor value of 2.005 to 2.011 equal to or greater than 10^{-8} mole/g of lyophilized tissue (at least in one of the four test samples of the same organ).

Decellularization of parenchymal and muscular intrathoracic organs can be considered effective in the absence of a signal with a g-factor in the range from 2.005 to 2.011 or a concentration of paramagnetic centers of less than 10^{-8} mole/g of lyophilized tissue in all four independent test samples of the same organ.

For the optimal detection of living cell systems capable of generating radicals characteristic of the electron transport chain in mitochondria, in the tissues of parenchymal and muscular intrathoracic organs, the following EPR-spectroscopy protocol can be recommended, including: preparation of four independent tissue samples from each studied object; followed by a sample preparation in which all samples should be lyophilized in a freeze dryer; further weighing the obtained lyophilized samples before measuring the EPR signal in a quartz ampoule of the EPR-spectrometer under the same conditions: at a temperature of 24°C in the X range (with the following measurement parameters: ultrahigh-frequency radiation – 1 mW, microwave frequency – 9144 MHz, amplitude of high-frequency modulation – 0.1 mT); after that the integral intensity of the EPR signal of the samples under investigation is calculated (double numerical integration), and the concentration of paramagnetic centers in the lyophilized samples is determined by comparing the obtained signal with the signal of the standard sample, 2,2,6,6-Tetramethylpiperidine 1-oxyl (TEMPO) containing in our case $6.4 \cdot 10^{-7}$ mole of paramagnetic centers.

Another method that allows differentiating native, decellularized and recellularized tissues of parenchymal and muscular intrathoracic organs is chemoluminescence. Based on the results of the study, it was demonstrated that the native tissues of the heart and lung show a rather high antioxidant activity and are able to suppress the H_2O_2-induced chemoluminescence flash to a higher extent than the decellularized matrices of these organs.

It was established for the first time that the chemoluminescence plots of native and recellularized tissues of these organs significantly differ from the chemoluminescence plots of decellularized tissues, primarily by the values of the rSCF·dSCF index proposed by the authors, which was characterized by the regularity of the change: significantly increasing in the comparative series – the decellularized tissues<native tissues<recellularized tissues, which allows to recommend it as one of the main criteria for evaluating the effectiveness of both decellularization and recellularization. At this, the above-mentioned regularity does not change even after processing of decellularized and recellularized lung tissues with chlorhexidine.

Acknowledgements

The investigation was carried out under the support of the complex research project 'Cell mechanisms of intrathoracic organs and tissues regeneration. Development of tissue-engineered constructs using biological and synthetic scaffolds', and under the support of the state assignment of the Ministry of Education and Science of the Russian Federation, project No. 6.5882.2017.

References

Badylak SF, Taylor D and Uygun K 2011 Whole-organ tissue engineering: decellularization and recellularization of three-dimensional matrix scaffolds. *Annu. Rev. Biomed. Eng.* **13** 27–53

Bleier L and Dröse S 2013 Superoxide generation by complex III: from mechanistic rationales to functional consequences. *Biochim. Biophys. Acta* **1827** 1320–1331

Brand MD 2010 The sites and topology of mitochondrial superoxide production. *Exp. Gerontol.* **45** 466–472

Conconi MT, De Coppi P, Bellini S, Zara G, Sabatti M, Marzaro M, Zanon GF, Gamba PG, Parnigotto PP and Nussdorfer GG 2005 Homologous muscle acellular matrix seeded with autologous myoblasts as a tissue-engineering approach to abdominal wall-defect repair. *Biomaterials* **26** 2567–2574

Daneshgar N, Rezaei M, Goudarzi M and Babadi N 2016 The ameliorative effect of naringenin on paraquat-induced toxicity in mitochondria isolated from rats. *Jundishapur J. Nat. Pharm. Prod.* **11** 32968

Dzhatdoeva AA, Polimova AM, Proskurnina EV and Vladimirov YuA 2016 Tissue chemiluminescence as a method of evaluation of superoxide radical producing ability of mitochondria. *Bull. Russ. State Med. Univ.* **1** 49–55

Frey BM, Zeisberger SM, Hoerstrup SP 2016 Tissue engineering and regenerative medicine-new initiatives for individual treatment offers. *Transfusion Med. Hemothe.* **43** 318–319

Gauthier JM, Ruiz-Pérez D, Li W, Hachem RR, Puri V, Gelman AE and Kreisel D. 2018 Diagnosis, pathophysiology and experimental models of chronic lung allograft rejection. *Transplantation* **102** 1459–1466

Gubareva EA, Sjöqvist S, Gilevich IV, Sotnichenko AS, Kuevda EV, Lim ML, Feliu N, Lemon G, *et al.* 2016 Orthotopic transplantation of a tissue engineered diaphragm in rats. *Biomaterials* **77** 320–335

Ito S and Hyodo F 2016 Dynamic nuclear polarization-magnetic resonance imaging at low ESR irradiation frequency for ascorbyl free radicals. *Sci. Rep.* **19** 21407

King MS, Sharpley MS and Hirst J 2009 Reduction of hydrophilic ubiquinones by the flavin in mitochondrial NADH: ubiquinone oxidoreductase (complex I) and production of reactive oxygen species. *Biochemistry* **48** 2053–2062

Kishikawa N, Ohkubo N, Ohyama K, Nakashima K and Kuroda N 2009 Chemiluminescence assay for quinones based on generation of reactive oxygen species through the redox cycle of quinone. *Anal. Bioanal. Chem.* **393** 1337–1343

Kőszegi T, Sali N, Raknić M, Horváth-Szalai Z, Csepregi R, Končić MZ, Papp N and Poór M 2017 A novel luminol-based enhanced chemiluminescence antioxidant capacity microplate assay for use in different biological matrices. *J. Pharmacol. Toxicol. Methods* **88** 153–159

Kuevda E, Gubareva E and Gilevich I 2013 Best decellularization protocol for tissue-engineered lungs. Proceedings of the world conference on regenerative medicine. *Regenerative Med.* **8** 21

Kuevda EV, Gubareva EA, Krasheninnikov SV, Grigoriev TE, Gumenyuk IS, Sotnichenko AS, Gilevich IV, Karal-Ogly DD, *et al.* 2016 Evaluation of the influence of decellularization on the changes in biomechanical properties of primate lungs. *Dokl. Biochem. Biophys.* **470** 375–378

Kuksal N, Chalker J and Mailloux RJ 2017 Progress in understanding the molecular oxygen paradox - function of mitochondrial reactive oxygen species in cell signaling. *Biol. Chem.* **398** 1209–1227

Liu L, He C, Liu J, Lv Z, Wang G, Gao H, Dai Y, Cooper DKC, Cai Z and Mou L 2018 Transplant tolerance: current insights and strategies for long-term survival of xenografts. *Arch. Immunol. Ther. Exp.* **66** 355–364

Mahla RS 2016 Stem cells applications in regenerative medicine and disease therapeutics. *Int. J. Cell Biol.* **2016** 6940283.

Maulucci G, Bačić G, Bridal L, Schmidt HH, Tavitian B, Viel T, Utsumi H, Yalçın AS and De Spirito M 2016 Imaging reactive oxygen species-induced modifications in living systems. *Antioxid. Redox. Signal.* **24** 939–958

Nastase M-V, Janicova A, Wygrecka M and Schaefer L 2017 Signaling at the crossroads: Matrix-derived proteoglycan and reactive oxygen species signaling. *Antioxid. Redox. Signal.* **27** 855–873

Orr AL, Vargas L, Turk CN, Baaten JE, Matzen JT, Dardov VJ, Attle SJ, Li J, *et al.* 2015 Suppressors of superoxide production from mitochondrial complex III. *Nat. Chem. Biol.* **11** 834–836

Ott HC, Matthiesen TS, Goh SK, Black LD, Kren SM, Netoff TI and Taylor DA 2008 Perfusion-decellularized matrix: using nature's platform to engineer a bioartificial heart. *Nat. Med.* **14** 213–221

Ott HC, Clippinger B, Conrad C, Schuetz C, Pomerantseva I, Ikonomou L, Kotton D and Vacanti JP 2010 Regeneration and orthotopic transplantation of a bioartificial lung. *Nat. Med.* **16** 927–933

Psaltis PJ, Peterson KM, Xu R, Franchi F, Witt T, Chen IY, Lerman A, Simari RD, Gambhir SS and Rodriguez-Porcel M 2013 Noninvasive monitoring of oxidative stress in transplanted mesenchymal stromal cells. *JACC Cardiovasc. Imaging* **6** 795–802

Rafati A, Taj SH, Azarpira N, Zarifkar A, Noorafshan A and Najafizadeh P 2011 Chronic morphine consumption increase allograft rejection rate in rat through inflammatory reactions. *Iran. Biomed. J.* **15** 85–91

Rackham CL and Jones PM 2018 Potential of mesenchymal stromal cells for improving islet transplantation outcomes. *Curr. Opin. Pharmacol.* **43** 34–39

Rezende F, Prior KK, Löwe O, Wittig I, Strecker V, Moll F, Helfinger V, Schnütgen F, *et al.* 2017 Cytochrome P450 enzymes but not NADPH oxidases are the source of the NADPH-dependent lucigenin chemiluminescence in membrane assays. *Free Radic. Biol. Med.* **102** 57–66

Sellaro TL, Ravindra AK, Stolz DB and Badylak SF 2007 Maintenance of hepatic sinusoidal endothelial cell phenotype in vitro using organ-specific extracellular matrix scaffolds. *Tissue Eng.* **13** 2301–2310

Sehati N, Kokhaei P, Ardekani AM, Tootoonchian R and Pak F 2017 Evaluation of serum interleukin-21 and HLA-C1 polymorphism in pediatrician hematopoietic stem cell transplantation for early diagnosis of acute graft-versus-host disease. *Iran. Biomed. J.* **21** 392–399

Sotnichenko AS, Gubareva EA and Gilevich IV 2013 Decellularized rat heart matrix as a basis for creation of tissue engineered heart. *Cell. Transplant. Tissue Eng.* **8** 86–94

Sozarukova MM, Polimova AM, Proskurnina EV and Vladimirov YA 2016 Changes in the kinetics of plasma chemiluminescence as a measure of systemic oxidative stress in humans. *Biophysics* **61** 284–290

Stockwell BR, Friedmann Angeli JP, Bayir H, Bush AI, Conrad M, Dixon SJ, Fulda S, Gascón S, *et al.* 2017 Ferroptosis: a regulated cell death nexus linking metabolism, redox biology, and disease. *Cell* **171** 273–285

Zhang Y and Weiner JH 2014 Characterization of the kinetics and electron paramagnetic resonance spectroscopic properties of *Acidithiobacillus ferrooxidans* sulfide: quinone oxidoreductase (SQR). *Arch. Biochem. Biophys.* **564** 110–119

Vladimirov YA and Proskurnina EV 2009 Free radicals and cell chemiluminescence. *Biochemistry* **74** 1545–1566

Vladimirov YA, Proskurnina EV and Izmajlov DY 2011 Kinetic chemiluminescence as a method for study of free radical reactions. *Biophysics* **56** 1055–1062

Wainwright JM, Czajka CA, Patel UB, Freytes DO, Tobita K, Gilbert TW and Badylak SF 2010 Preparation of cardiac extracellular matrix from an intact porcine heart. *Tissue Eng. C Methods.* **16** 525–532

Wang D, Zhao L, Ma H, Zhang H and Guo LH 2017 Quantitative analysis of reactive oxygen species photogenerated on metal oxide nanoparticles and their bacteria toxicity: the role of superoxide radicals. *Environ. Sci. Technol.* **51** 10137–10145

Wang Y 2016 Understanding Ubiquinone. *Trends Cell Biol.* **26** 367–378

Yamamoto K, Ikenaka Y, Ichise T, Bo T, Ishizuka M, Yasui H, Hiraoka W, Yamamori T and Inanami O 2018 Evaluation of mitochondrial redox status and energy metabolism of X-irradiated HeLa cells by LC/UV, LC/MS/MS and ESR. *Free Radic. Res.* **52** 648–660

Corresponding editor: BJ Rao